

Ages and Metallicities in Elliptical Galaxies from the H_β , $\langle\text{Fe}\rangle$, and Mg_2 Diagnostics

Rosaria Tantalo¹, Cesare Chiosi^{2,1}, Alessandro Bressan³

¹ Department of Astronomy, Vicolo dell' Osservatorio 5, 35122 Padua, Italy

² European Southern Observatory, K-Schwarzschild-strasse 2, D-85748, Garching bei Muenchen, Germany

³ Astronomical Observatory, Vicolo dell' Osservatorio 5, 35122 Padua, Italy

Received: November 1997. Accepted:

Abstract. Systematic variations in the line strength indices H_β , Mg_2 , and $\langle\text{Fe}\rangle$ are observed across elliptical galaxies and limited to the central regions passing from one object to another. Furthermore, since the gradients in Mg_2 and $\langle\text{Fe}\rangle$ have often different slopes arguments are given for an enhancement of Mg (α -elements in general) with respect to Fe toward the center of these galaxies. Finally, the inferred degree of enhancement seems to increase passing from dwarfs to massive ellipticals.

In this study we have investigated the ability of the H_β , Mg_2 and $\langle\text{Fe}\rangle$ diagnostics to assess the metallicity, $[\text{Mg}/\text{Fe}]$ ratios, and ages of elliptical galaxies.

To this aim, first we derive basic calibrations for the variations δH_β , δMg_2 and $\delta \langle\text{Fe}\rangle$ as a function of variation in age $\Delta \log(t)$, metallicity $\Delta \log(Z/Z_\odot)$, and $\Delta [\text{Mg}/\text{Fe}]$.

Second, examining the gradients observed in a small sample of galaxies, we analyze how the difference δH_β , δMg_2 , and $\delta \langle\text{Fe}\rangle$ between the external and central values of each index translates into $\Delta [\text{Mg}/\text{Fe}]$, $\Delta \log(Z/Z_\odot)$, and $\Delta \log(t)$. We find that out of six galaxies under examination, four have the nuclear region more metal-rich, more enhanced in α -elements, and younger (i.e. containing a significant fraction of stars of relatively young age) than the external regions. In contrast the remaining two galaxies have the nuclear region more metal-rich, more enhanced in α -elements but marginally older than the external zones.

Third, we explore the variation from galaxy to galaxy of the nuclear values of H_β , Mg_2 , and $\langle\text{Fe}\rangle$ limited to a sub-sample of the Gonzales (1993) list. The differences δH_β , δMg_2 , and $\delta \langle\text{Fe}\rangle$ are converted into the differences $\Delta \log(t)$, $\Delta \log(Z/Z_\odot)$, and $\Delta [\text{Mg}/\text{Fe}]$. Various correlations among the age, metallicity, and enhancement variations are explored. In particular we thoroughly examine the relationships $\Delta \log(t) - M_V$, $\Delta \log(Z/Z_\odot) - M_V$, and $\Delta [\text{Mg}/\text{Fe}] - M_V$. It is found that a sort of age limit is likely to exist in the $\Delta \log(t) - M_V$ plane, traced by

galaxies with mild or no sign of rejuvenation. In these objects, the duration of the star forming activity is likely to have increased at decreasing galactic mass. Limited to these galaxies, the mass-metallicity sequence implied by the color-magnitude relation is recovered, likewise for the α -enhancement-luminosity relation suggested by the gradients in Mg_2 and $\langle\text{Fe}\rangle$. For the remaining galaxies the situation is more intriguing: sporadic episodes of star formations are likely to have occurred scattering the galaxies in the space of age (H_β), metallicity, and $[\text{Mg}/\text{Fe}]$.

The results are discussed in regard to predictions from the merger and isolation models of galaxy formation and evolution highlighting points of difficulty with each scheme. Finally, the suggestion is advanced that models with an IMF that at the early epochs favors higher mass stars in massive ellipticals galaxies, and lower mass stars in low-mass ellipticals, might be able to alleviate some of the difficulties encountered by the standard SN-driven galactic wind model and lead to a coherent interpretation of the data.

Key words: Galaxies: line strength indices – Galaxies: stellar content – Galaxies: ellipticals – Galaxies: ages

1. Introduction

Elliptical galaxies exhibit systematic variations in the line strength indices H_β , Mg_2 , and $\langle\text{Fe}\rangle$ either going from the center to the external regions of a galaxy or limited to the central regions passing from one galaxy to another. (cf. Gonzales 1993; Carollo & Danziger 1994a,b; Carollo et al. 1993; Davies et al. 1993; Fisher et al. 1995, 1996). Furthermore, since the gradients in Mg_2 and $\langle\text{Fe}\rangle$ have different slopes arguments are given for an enhancement of Mg (α -elements in general) with respect to Fe toward the center of these galaxies. Finally, the inferred degree

of enhancement seems to increase passing from dwarfs to massive ellipticals (see Faber et al. 1992, Worthey et al. 1994 and Matteucci 1997 for recent reviews of all these subjects and exhaustive referencing).

All this suggests the occurrence of changes in some fundamental properties of the constituent stellar populations. The understanding of this problem is that either the age or the metallicity (the abundance pattern, in general) or both are likely to be responsible for the above variations.

Owing to the primary importance of ranking galaxies (or regions of these) as function of the age, metallicity and abundance ratios in regard to the more general subject of galaxy formation and evolution, in this paper we present a new attempt aimed at unraveling the information contained in the indices H_β , Mg_2 , and $\langle Fe \rangle$ for a sample of elliptical galaxies.

The above indices have complicated dependences on the temperature, gravity, and chemical abundances of the emitting stars, cf. the popular empirical calibrations by Worthey (1992), Worthey et al. (1994) and Borges et al. (1995). When these calibration are applied to derive the mean value of the indices in question for single stellar populations (SSP) as a function of the age and chemical abundances, the results suffer from a certain degree of degeneracy in the sense that all the indices vary in the same way at varying age and chemical composition, the well known *age-metallicity degeneracy* (cf. Worthey 1994). Furthermore, when the last step is undertaken, i.e. the above indices are derived for complex assemblies of stars of any age and composition, interpreting the observational data is even more intrigued because the indices are found to depend on the underlying relative distribution of stars per metallicity bin, i.e. the so-called partition function $N(Z)$ introduced by Tantalo et al. (1997) in their analysis of this problem. This means that hints on the past history of star formation are needed to solve the problem.

Despite these intrinsic difficulties H_β , Mg_2 , and $\langle Fe \rangle$ respond in different fashion to different parameters: H_β mainly correlates with the age because it is most sensitive to the light emitted by stars at the turnoff, whereas Mg_2 and $\langle Fe \rangle$ are more related to stars along the RGB and therefore are more sensitive to metallicity and abundance ratios (cf. Worthey 1994). Therefore, an attempt to infer age, metallicity, and abundance ratios from these line strength indices is possible.

The plan of the paper is as follows. In section 2 we briefly recall the sources of data we have adopted in this study. In section 3 we derive new basic relationships providing the variation of H_β , Mg_2 , and $\langle Fe \rangle$ in SSPs (from which eventually the galactic indices are built up) as a function of age t , total metallicity Z , and $[Mg/Fe]$, and in section 4 we present the Δ -method. In section 5, we apply out diagnostics to study the gradients in Mg_2 and $\langle Fe \rangle$ across elliptical galaxies limited to a small number of objects for which the data were available. In section 6, we study the variations of nuclear values of H_β , Mg_2

and $\langle Fe \rangle$ from galaxy to galaxy of the Gonzales (1993) sample and translate these variations into differences in age, metallicity, and enhancement of α -elements. In section 7, we thoroughly examine the galaxies in the space of $\Delta \log(t)$, $\Delta \log(Z/Z_\odot)$, and $\Delta[Mg/Fe]$, where Δ stands for the difference between the values of the three quantities for each individual object and their mean values in the sample. In section 8 we attempt a preliminary ranking of the galaxies as a function of their absolute age, metallicity, and $[Mg/Fe]$. In section 9 we discuss the results of the analysis in regard to the present-day understanding of the mechanism of formation and evolution of elliptical galaxies: i.e. isolation or merger. In section 10 we compare the results with the predictions from the SN-driven galactic wind both at constant and variable IMF. Finally, some concluding remarks are drawn in section 11.

2. The observational data

There are several sources of data that are useful to our purposes:

- The fully corrected indices of Gonzales (1993) for two different galaxy coverage. The central region within $Re/8$ (Re is the effective radius), the wider area within $Re/2$, and finally the *nuclear region* within 2×4.1 arc-sec. In the same source there are high quality gradient data for some 20 galaxies. The Gonzales (1993) list of nuclear data is used to study the variations in the indices from galaxy to galaxy.
- The small sample of ellipticals by Carollo & Danziger (1994a,b) containing detailed data for gradients in Mg_2 and $\langle Fe \rangle$. This sample is utilized to illustrate the capability of the method when applied to individual galaxies, and to perform a preliminary analysis of the gradient in age, metallicity and ratio $[Mg/Fe]$ in individual objects.
- The samples by Davies et al. (1993) and Fisher et al. (1995, 1996) containing data on 13 and 7 elliptical respectively, and finally galaxies by Vazdekis (1997, private communication). The results for these data sets are not shown here for the sake of brevity. They have been separately used to check whether results obtained with the other sets were also confirmed by these ones.

No attempt is made to put all these data sources together, because we feel that manipulating the data to render all sources mutually consistent (it is worth recalling that each sample differs from the others in many observational details: galaxy coverage, reduction technique, calibrations, etc..) would introduce spurious effects difficult to handle. For these reasons we prefer to use smaller albeit homogeneous sets of data. It is beyond the aims of this study to perform a systematic analysis of all data in literature. We anticipate that the results obtained from using separately each sub-group of data are in mutual agreement.

3. Calibrations containing [Mg/Fe]

Many studies have emphasized that line strength indices depend not only on the stellar parameters T_{eff} , gravity, and [Fe/H] as in the classical calibration by Worthey (1992) and Worthey et al. (1994), but also on the ratios of chemical abundances such as [Mg/Fe] in particular (Barbuy 1994, Idiart et al. 1995, Weiss et al. 1995, Borges et al. 1995, de Freitas & Pacheco 1997, Idiart & de Freitas Pacheco 1997). Needless to say that for the purposes of this study we have to adopt calibrations in which the ratio [Mg/Fe] is taken into account.

We start pointing out that in presence of a certain degree of enhancement in α -elements one has to suitably modify relationship between the total metallicity Z and the iron content [Fe/H]. Using the pattern of abundances by Anders & Grevesse (1989), Grevesse (1991) and Grevesse & Noels (1993), we find the general relation

$$\left[\frac{\text{Fe}}{\text{H}}\right] = \log\left(\frac{Z}{Z_{\odot}}\right) - \log\left(\frac{X}{X_{\odot}}\right) - 0.8 \left[\frac{\alpha}{\text{Fe}}\right] - 0.05 \left[\frac{\alpha}{\text{Fe}}\right]^2 \quad (1)$$

where the term $[\alpha/\text{Fe}]$ stands for all α -elements lumped together.

The recent empirical calibration by Borges et al. (1995) for the Mg_2 index includes the effect of different [Mg/Fe] ratios

$$\ln \text{Mg}_2 = -9.037 + 5.795 \frac{5040}{T_{\text{eff}}} + 0.398 \log g + 0.389 \left[\frac{\text{Fe}}{\text{H}}\right] - 0.16 \left[\frac{\text{Fe}}{\text{H}}\right]^2 + 0.981 \left[\frac{\text{Mg}}{\text{Fe}}\right] \quad (2)$$

which holds for effective temperatures and gravities in the ranges $3800 < T_{eff} < 6500$ K and $0.7 < \log g < 4.5$.

To our knowledge, no corresponding calibrations for H_{β} and $\langle \text{Fe} \rangle$ are yet available, so that one is forced to adopt those by Worthey et al. (1994) with no dependence on [Mg/Fe]. Nevertheless, a zero-order evaluation of the effect of [Mg/Fe] on H_{β} and $\langle \text{Fe} \rangle$ is possible via the different relation between Z and [Fe/H] of the $[\alpha/\text{Fe}] \neq 0$ case (cf. Tantalo et al 1997 for more details).

With the aid of the relations above for [Fe/H], Mg_2 and implicitly H_{β} and $\langle \text{Fe} \rangle$ are used to generate new SSPs in which not only the chemical abundances are enhanced with respect to the solar value but also the effect of this on the line strength indices is taken into account in a self-consistent manner.

The procedure is as follows: assumed the total metallicity Z and enhancement ratio [Mg/Fe] as input parameters for the chemical abundances, we derive from eq. (1) the corresponding value of [Fe/H] to be inserted in the calibrations of Borges et al. (1995) for Mg_2 (eq. 2), and Worthey (1992) and Worthey et al. (1994) for $\langle \text{Fe} \rangle$ and H_{β} . The helium content Y associated to each value of Z is the same as in the standard SSP of Bertelli et al. (1994).

Table 1 lists a summary of the parameters characterizing each SSP and their Mg_2 , $\langle \text{Fe} \rangle$ and H_{β} for four values of age (15, 10, 5, and 1 Gyr).

It is worth clarifying that these SSPs are calculated with the stellar models of the Padua library (Bertelli et al. 1994) in which $[\alpha/\text{Fe}] = 0$. Although full consistency would require that the stellar models in usage had the same abundance ratios as the SSPs above, neglecting this has very marginal consequences as models calculated with the new opacity tables of the Livermore group (Iglesias & Rogers 1993), in which the enhancement of the α -elements is taken into account, and the re-definition of [Fe/H] at given Z and [Mg/Fe] are virtually indistinguishable in the CMD from the old ones (Bressan et al. 1997). The marginal variation in the lifetime of the core H-burning phase can be ignored for all practical purposes.

Table 1. New SSPs with different metallicity and [Mg/Fe].

Age(Gyr)	Z	[Mg/Fe]	[Fe/H]	Mg_2	$\langle \text{Fe} \rangle$	H_{β}
15	0.004	+0.3	-0.952	0.134	1.714	1.687
15	0.004	0.0	-0.707	0.125	1.931	1.710
15	0.004	-0.3	-0.472	0.115	2.165	1.750
15	0.02	+0.3	-0.214	0.262	2.787	1.312
15	0.02	0.0	+0.031	0.229	3.087	1.377
15	0.02	-0.3	+0.266	0.198	3.395	1.452
15	0.05	+0.3	+0.253	0.365	3.606	1.197
15	0.05	0.0	+0.497	0.308	3.937	1.279
15	0.05	-0.3	+0.733	0.258	4.276	1.368
10	0.004	+0.3	-0.952	0.126	1.609	1.884
10	0.004	0.0	-0.707	0.116	1.839	1.910
10	0.004	-0.3	-0.472	0.106	2.084	1.954
10	0.02	+0.3	-0.214	0.243	2.649	1.489
10	0.02	0.0	+0.031	0.212	2.949	1.556
10	0.02	-0.3	+0.266	0.183	3.262	1.629
10	0.05	+0.3	+0.253	0.357	3.503	1.312
10	0.05	0.0	+0.497	0.300	3.840	1.393
10	0.05	-0.3	+0.733	0.250	4.184	1.483
5	0.004	+0.3	-0.952	0.104	1.401	2.388
5	0.004	0.0	-0.707	0.097	1.630	2.415
5	0.004	-0.3	-0.472	0.090	1.875	2.455
5	0.02	+0.3	-0.214	0.211	2.431	1.884
5	0.02	0.0	+0.031	0.182	2.734	1.945
5	0.02	-0.3	+0.266	0.155	3.050	2.018
5	0.05	+0.3	+0.253	0.308	3.235	1.648
5	0.05	0.0	+0.497	0.255	3.584	1.734
5	0.05	-0.3	+0.733	0.210	3.943	1.828
1	0.004	+0.3	-0.952	0.051	0.659	4.819
1	0.004	0.0	-0.707	0.046	0.823	4.819
1	0.004	-0.3	-0.472	0.042	1.015	4.831
1	0.02	+0.3	-0.214	0.101	1.562	4.018
1	0.02	0.0	+0.031	0.093	1.856	4.074
1	0.02	-0.3	+0.266	0.085	2.166	4.140
1	0.05	+0.3	+0.253	0.161	2.377	3.758
1	0.05	0.0	+0.497	0.142	2.731	3.532
1	0.05	-0.3	+0.733	0.127	3.100	3.631

4. The δH_β , δMg_2 , and $\delta \langle \text{Fe} \rangle$ method

In this section we present the tool utilized to transfer variations in H_β , Mg_2 , and $\langle \text{Fe} \rangle$ into variations in age (t), metallicity (Z), and $[\text{Mg}/\text{Fe}]$. To this purpose we calculate the partial derivatives ∂Mg_2 , $\partial \langle \text{Fe} \rangle$ and ∂H_β with respect to metallicity, age, and $[\text{Mg}/\text{Fe}]$ of SSPs

$$\begin{aligned} \frac{\partial \text{Mg}_2}{\partial \log Z/Z_\odot} \Big|_{t, [\frac{\text{Mg}}{\text{Fe}}]} & \quad \frac{\partial \text{Mg}_2}{\partial [\text{Mg}/\text{Fe}]} \Big|_{t, Z} & \quad \frac{\partial \text{Mg}_2}{\partial \log t} \Big|_{Z, [\frac{\text{Mg}}{\text{Fe}}]} \\ \frac{\partial \langle \text{Fe} \rangle}{\partial \log Z/Z_\odot} \Big|_{t, [\frac{\text{Mg}}{\text{Fe}}]} & \quad \frac{\partial \langle \text{Fe} \rangle}{\partial [\text{Mg}/\text{Fe}]} \Big|_{t, Z} & \quad \frac{\partial \langle \text{Fe} \rangle}{\partial \log t} \Big|_{Z, [\frac{\text{Mg}}{\text{Fe}}]} \\ \frac{\partial H_\beta}{\partial \log Z/Z_\odot} \Big|_{t, [\frac{\text{Mg}}{\text{Fe}}]} & \quad \frac{\partial H_\beta}{\partial [\text{Mg}/\text{Fe}]} \Big|_{t, Z} & \quad \frac{\partial H_\beta}{\partial \log t} \Big|_{Z, [\frac{\text{Mg}}{\text{Fe}}]} \end{aligned}$$

together with their uncertainties due to the small deviations of the various quantities over the range of age, Z , and $[\text{Mg}/\text{Fe}]$ spanned by the calibrating SSPs (cf. the entries of Table 1).

The mean variation δMg_2 , $\delta \langle \text{Fe} \rangle$ and δH_β as a function of $[\text{Mg}/\text{Fe}]$, $\log(Z/Z_\odot)$, and $\log(t)$, where $Z_\odot = 0.016$ and ages are Gyr, are cast as follows

$$\begin{aligned} \delta \text{Mg}_2 = & 0.0994(\pm 0.0003) \times \Delta \left[\frac{\text{Mg}}{\text{Fe}} \right] \\ & + 0.1660(\pm 0.0299) \times \Delta \log \left(\frac{Z}{Z_\odot} \right) \\ & + 0.0889(\pm 0.0047) \times \Delta \log(t) \end{aligned} \quad (3)$$

$$\begin{aligned} \delta \langle \text{Fe} \rangle = & -0.9806(\pm 0.0003) \times \Delta \left[\frac{\text{Mg}}{\text{Fe}} \right] \\ & + 1.8743(\pm 0.2637) \times \Delta \log \left(\frac{Z}{Z_\odot} \right) \\ & + 0.7021(\pm 0.0079) \times \Delta \log(t) \end{aligned} \quad (4)$$

$$\begin{aligned} \delta H_\beta = & -0.2097(\pm 0.0016) \times \Delta \left[\frac{\text{Mg}}{\text{Fe}} \right] \\ & - 0.4837(\pm 0.0937) \times \Delta \log \left(\frac{Z}{Z_\odot} \right) \\ & - 1.2070(\pm 0.0084) \times \Delta \log(t) \end{aligned} \quad (5)$$

These equations are referred to as the Δ -method.

To visually show the size of $\delta \langle \text{Fe} \rangle$ and δMg_2 at varying $[\text{Mg}/\text{Fe}]$, Z , and $\log(t)$, we calculate the *age*, *metallicity*, and *enhancement vectors* shown in Fig. 1 for fixed

variations of age, metallicity, and $[\text{Mg}/\text{Fe}]$: the age goes from 5 to 15 Gyr, the metallicity from 0.004 to 0.05, and the $[\text{Mg}/\text{Fe}]$ ratio from -0.3 to 0.4 dex (the length of the vectors is $\Delta \log(Z) \sim 1.1$, $\Delta [\text{Mg}/\text{Fe}] \sim 0.7$ and $\Delta \log(t) \sim 0.47$). The vectors are centered on $(0,0)$, i.e. null variation.

There are two important points to remark:

- The well known age-metallicity degeneracy given that the age and metallicity vectors run very close each other.
- The enhancement vector is almost orthogonal to the other two, which allows us to separate its effects from the combined ones of age and metallicity.

Finally, concluding this section we like to recast the system of equations (3) through (5) so that the theoretical $[\text{Mg}/\text{Fe}]$, $\log(Z/Z_\odot)$, and $\log(t)$ are expressed as a function of the observational mean variations δMg_2 , $\delta \langle \text{Fe} \rangle$ and δH_β

$$\begin{aligned} \Delta [\text{Mg}/\text{Fe}] = & 5.7410 \times \delta \text{Mg}_2 - 0.4699 \times \delta \langle \text{Fe} \rangle \\ & + 0.1495 \times \delta H_\beta \end{aligned} \quad (6)$$

$$\begin{aligned} \Delta \log \left(\frac{Z}{Z_\odot} \right) = & 3.9738 \times \delta \text{Mg}_2 + 0.3026 \times \delta \langle \text{Fe} \rangle \\ & + 0.4687 \times \delta H_\beta \end{aligned} \quad (7)$$

$$\begin{aligned} \Delta \log(t) = & -2.5899 \times \delta \text{Mg}_2 - 0.0396 \times \delta \langle \text{Fe} \rangle \\ & - 1.0424 \times \delta H_\beta \end{aligned} \quad (8)$$

The solutions of these equations are known with the following uncertainty: $\Delta [\text{Mg}/\text{Fe}] \pm 0.0890$, $\Delta \log(Z/Z_\odot) \pm 0.1524$, and $\Delta \log(t) \pm 0.0538$. However, the analysis below will make use of the first original formulation because of its better accuracy.

5. Gradients across individual galaxies

In this section we study the gradients in H_β , Mg_2 , and $\langle \text{Fe} \rangle$ across a few individual galaxies. The analysis is made in two steps.

We start showing in Fig. 1 the data for four galaxies taken from different sources, namely NGC 4472 from Davies et al. (1993), NGC 4594 from Vazdekis (1997, private communication), and NGC 2434 and NGC 3706 from Carollo & Danziger (1994a,b). Galaxies have been chosen on the base of the following criteria: elliptical objects and enough data per galaxy. This first step is meant to illustrate the method.

The displayed data are the difference between the local value of each index (at any radial distance) and its value at the center. Taking the galaxy NGC 4594 as a prototype, we first derive an eye estimate of the mean slope of the data, second we translate the origin of the vectors

to some arbitrary external point of the galaxy. The result is that with respect to its external regions, the nucleus is either more metal-rich and older or more metal-rich and slightly younger, and in any case more enhanced in $[\text{Mg}/\text{Fe}]$. It goes without saying that if the nucleus is older than the periphery a lower increase in the metallicity toward the center is required than in the opposite alternative (younger nucleus). In such a case the increase in metallicity must be large enough to compensate for the opposite trend of the age. Similar considerations apply also to the other galaxies in Fig. 1.

How this result conforms to the Bressan et al. (1996) analysis of Gonzales (1993) galaxies in the H_β and $[\text{Mg}/\text{Fe}]$, suggesting that in most galaxies the nucleus is younger (star formation lasted longer) and more metal-rich than the external regions, with a minority having the nucleus older and more metal-rich ?

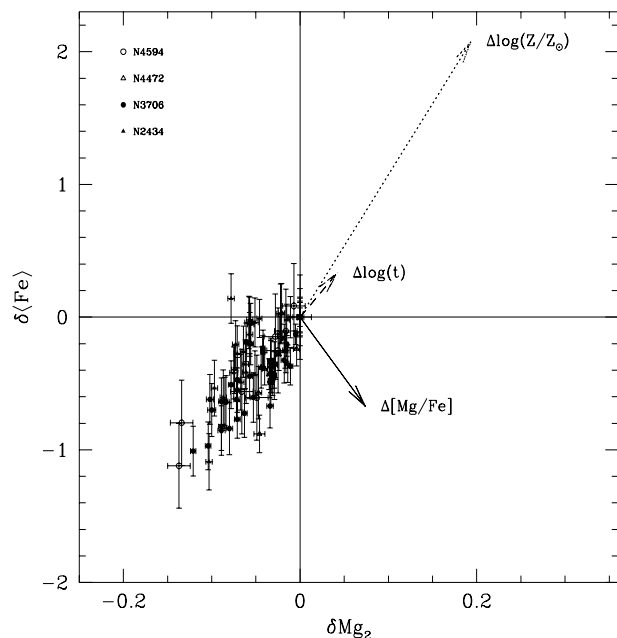


Fig. 1. The $\delta\langle\text{Fe}\rangle$ versus δMg_2 relation. The three arrows centered on (0,0) indicate the *age*, *metallicity*, and *enhancement* vectors as indicated. Along the age vector, the age goes from 5 to 15 Gyr, along the metallicity vector Z ranges from 0.004 to 0.05, and along the enhancement vector $[\text{Mg}/\text{Fe}]$ goes from -0.3 to 0.4 dex. The data are from Vazdekis (1997, private communication) for NGC 4594, from Davies et al. (1993) for NGC 4472, and from Carollo & Danziger (1994a) for NGC 2434 and NGC 3706.

To answer the above question we make use of the H_β index, known to be more sensitive to the age, and look at the parameter space H_β , Mg_2 and $\langle\text{Fe}\rangle$.

In Fig. 2 the same type of data as in Fig. 1 is shown, but in the δH_β versus δMg_2 plane, together with the the-

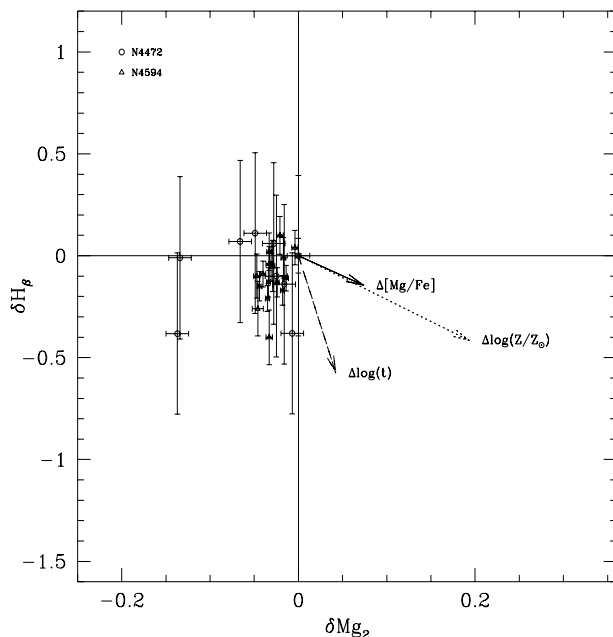


Fig. 2. The δH_β versus δMg_2 relation. The three arrows centered on (0,0) indicate the *age*, *metallicity*, and *enhancement* vectors as indicated. Along the age vector, the age goes from 5 to 15 Gyr, along the metallicity vector Z ranges from 0.004 to 0.05, and along the enhancement vector $[\text{Mg}/\text{Fe}]$ goes from -0.3 to 0.4 dex. The data are from Vazdekis (1997, private communication) for NGC 4594, and from Davies et al. (1993) for NGC 4472.

oretical age, metallicity, and $[\text{Mg}/\text{Fe}]$ vectors. Now the number of galaxies that are plotted is very small, only two objects indeed, namely NGC 4472 from Davies et al. (1993) and NGC 4594 from Vazdekis (1997, private communication). Two more galaxies from Davies et al. (1993) are not shown on Fig. 2 for the sake of clarity.

We learn from this diagram that the two galaxies in question have their nuclear region containing stars that are more enhanced in α -elements, more metal-rich, and younger than the external regions.

To strengthen the above preliminary conclusion we have repeated the analysis by means of the Δ -method. The galaxies under examinations are those already displayed in Figs. 1 and 2 plus NGC 3379 and NGC 4374 taken from Davies et al. (1993). The results are summarized in Table 2. The top part of the table shows the observational data, i.e. the mean values of Mg_2 , $\langle\text{Fe}\rangle$, and H_β of the central region (indicated by a capitol N) and the external region (labelled by a capitol E). The central region is defined by visually inspecting the Mg_2 gradient in the case of the Carollo & Danziger (1994a,b) objects (5 arcsec from the galactic centre) or taken according to the definition given by the authors for the remaining galaxies.

Table 2. Estimated gradients in age (Gyr), metallicity (Z/Z_\odot) and α -enhancement across a small group of galaxies. (1) Carollo & Danziger (1994a); (2) Davies et al. (1993); (3) Vazdekis (1997). See the text for more details.

NGC	Ref	Mg _{2N}	$\langle\text{Fe}\rangle_N$	H _{βN}	Mg _{2E}	$\langle\text{Fe}\rangle_E$	H _{βE}
2434	(1)	0.235	2.579	2.200	0.183	2.378	1.800
3706	(1)	0.292	2.937	1.800	0.232	2.584	1.800
3379	(2)	0.311	2.947	1.483	0.277	2.748	1.632
4374	(2)	0.318	2.900	1.263	0.289	2.683	1.494
4472	(2)	0.345	3.440	1.510	0.321	3.247	1.412
4594	(3)	0.332	3.102	1.183	0.212	1.974	0.943
NGC	Ref	δMg_2	$\delta\langle\text{Fe}\rangle$	δH_β	$\Delta[\frac{\text{Mg}}{\text{Fe}}]$	$\Delta\log(\frac{Z}{Z_\odot})$	$\Delta\log(t)$
2434	(1)	-0.052	-0.201	-0.400	-0.231	-0.409	0.500
3706	(1)	-0.060	-0.353	0.000	-0.154	-0.311	0.124
3379	(2)	-0.034	-0.199	0.149	-0.070	-0.112	-0.076
4374	(2)	-0.029	-0.217	0.231	-0.025	-0.066	-0.167
4472	(2)	-0.024	-0.193	-0.098	-0.048	-0.181	0.146
4594	(3)	-0.120	-1.146	-0.240	-0.126	-0.851	0.488

The bottom part of Table 2 lists the difference δMg_2 , $\delta\langle\text{Fe}\rangle$, and δH_β between the external and central values of the three indices, and the solution found for $\Delta[\text{Mg}/\text{Fe}]$, $\Delta\log(Z/Z_\odot)$, and $\Delta\log(t)$ between the periphery and centre.

It turns out that of the six galaxies, four have the nuclear region containing stars more enhanced in α -elements, more metal-rich, and younger than the external regions, whereas two of them have the nucleus more metal-rich, more α -enhanced but (marginally) older than the external regions.

6. Going from galaxy to galaxy

Given that the central values of H_β , Mg_2 , and $\langle\text{Fe}\rangle$ are known to vary from galaxy to galaxy, what the implications are as far as the differences in age, metallicity, and enhancement in α -elements are concerned?

To answer this question we make use of the Gonzales (1993) sample of elliptical galaxies (41 objects in total) containing the so-called *nuclear data*, i.e. within 2×4.1 arcsec. The data are presented in Table 3. Column (1) identifies the galaxy: those objects whose name is followed by a V belong to the Virgo cluster. Columns (2) to (5) give Mg_2 , Fe_{5270} and Fe_{5335} , and H_β . Columns (6), (7) and (8) show the differences δH_β , δMg_2 , and $\delta\langle\text{Fe}\rangle$ of the galaxy indices with respect to the mean values (see below), respectively. Columns (9), (10), and (11) give the difference with respect to the mean of the enrichment fac-

tor $\Delta[\text{Mg}/\text{Fe}]$, metallicity $\Delta\log(Z/Z_\odot)$, and age $\Delta\log(t)$ found for each galaxy. Columns (12) and (13) list the total absolute blue and visual magnitudes M_B and M_V , respectively. Finally, column (14) list the rejuvenation parameter Σ defined by Schweizer & Seitzer (1992). For each galaxy, the top row are the data (either observational or theoretical), whereas the bottom row are the corresponding uncertainties.

To perform the analysis we have calculated the mean values of Mg_2 , $\langle\text{Fe}\rangle$ and H_β for the whole sample: $\overline{\text{H}_\beta} = 1.75$, $\overline{\text{Mg}_2} = 0.32$, and $\overline{\langle\text{Fe}\rangle} = 2.96$.

They are used as the origin of a new system of coordinates in which the differences δMg_2 , $\delta\langle\text{Fe}\rangle$ and δH_β passing from galaxy to galaxy are expressed.

6.1. The δMg_2 - $\delta\langle\text{Fe}\rangle$ and δMg_2 - δH_β planes

The observational data for the differences δMg_2 and $\delta\langle\text{Fe}\rangle$ are shown in Fig. 3, in which we have drawn the metallicity, enhancement, and age vectors, whose length is the same as in the previous analysis, and finally indicated the positions of M32 and NGC 4649, the prototype galaxies in the discussion below. Once again, age and metallicity cannot be safely separated, whereas this is feasible for $[\text{Mg}/\text{Fe}]$.

In order to cope with the age-metallicity degeneracy encountered in the δMg_2 - $\delta\langle\text{Fe}\rangle$ plane, we look at the δMg_2 - δH_β plane owing to the better age sensitivity of H_β . This plane is shown in Fig. 4 where the module of the

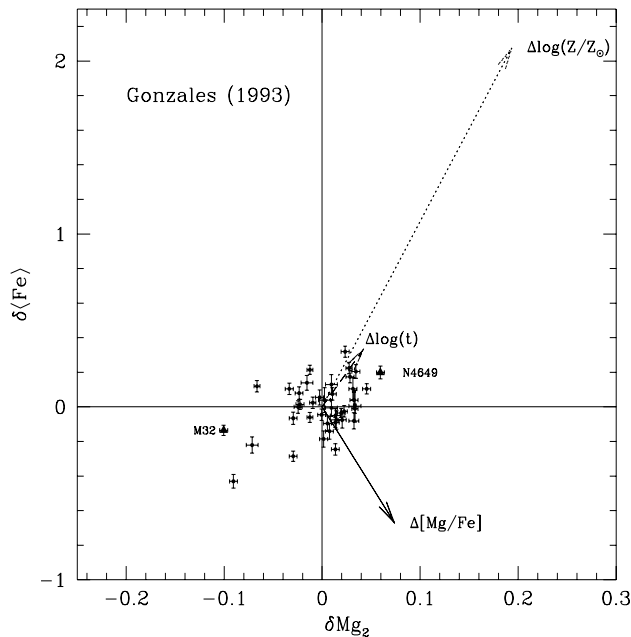


Fig. 3. The $\delta\langle\text{Fe}\rangle$ versus δMg_2 relation. The three arrows centered on (0,0) are the *age*, *metallicity*, and *enhancement vectors* as indicated. They have been calculated as in Fig.1. The displayed data are for each galaxy the difference between its central value and the mean value of the sample. The position of M32 and NGC 4649 is indicated.

three vectors are: $\Delta\log(Z) \sim 1.1$, $\Delta[\text{Mg}/\text{Fe}] \sim 0.7$ and $\Delta\log(t) \sim 0.47$. In this figure the effect of $[\text{Mg}/\text{Fe}]$ and metallicity cannot be isolated because the two vectors are coincident (degeneracy), whereas this is feasible for the age.

With the aid of the Δ -method and the differences δH_β , δMg_2 , and $\delta\langle\text{Fe}\rangle$, we derive for each galaxy the variations in age $\Delta\log(t)$, metallicity $\Delta\log(Z/Z_\odot)$, and enhancement $\Delta[\text{Mg}/\text{Fe}]$ with respect to the mean values. The results together with the expected uncertainties are listed in columns (9), (10) and (11) of Table 3.

Looking at M32 and NGC 4649 as an example, we get the following results: for M32 $\Delta\log(t) = -0.392$, $\Delta\log(Z/Z_\odot) = -0.131$, and $\Delta[\text{Mg}/\text{Fe}] = -0.403$; for NGC 4649 $\Delta\log(t) = 0.245$, $\Delta\log(Z/Z_\odot) = 0.106$, and $\Delta[\text{Mg}/\text{Fe}] = 0.180$. The stellar content of M32 is less metal rich, less enhanced in α -elements, and much younger (or more safely has a much younger component contributing to H_β) than NGC 4649.

7. The $\Delta\log(t)$, $\Delta\log(Z/Z_\odot)$, $\Delta[\text{Mg}/\text{Fe}]$ space

Aim of this section is to investigate whether systematic correlations exist among the three physical quantities $\Delta\log(t)$, $\Delta\log(Z/Z_\odot)$, and $\Delta[\text{Mg}/\text{Fe}]$. The occurrence of such relations would bear very much on the past history

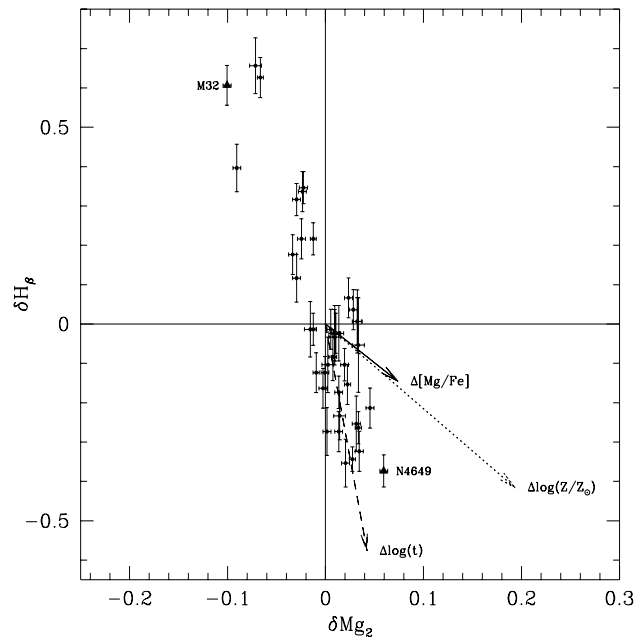


Fig. 4. The δH_β versus δMg_2 relation. The three arrows centered on (0,0) are the *age*, *metallicity* and *enhancement vectors* as indicated. They have been calculated as in Fig.2. The data are from Gonzales (1993) and for each galaxy the difference between its central values and the mean value of the sample are displayed. The position of M32 and NGC 4649 is indicated.

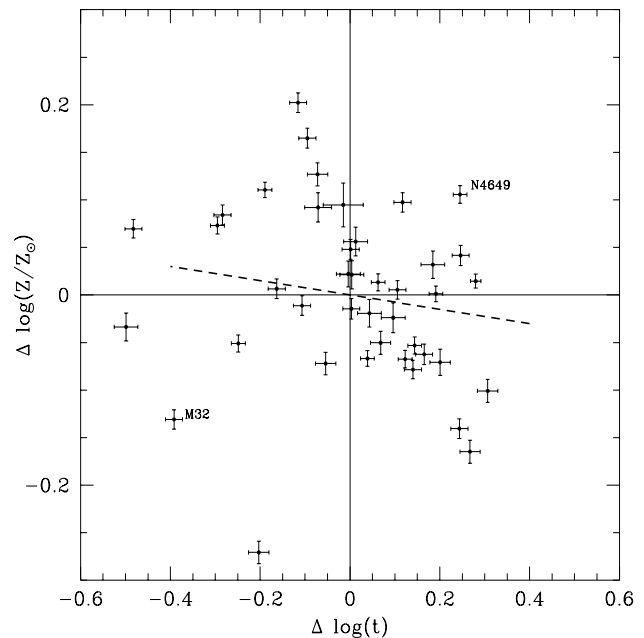


Fig. 5. The $\Delta\log(Z/Z_\odot)$ versus $\Delta\log(t)$ relation. The *thick dashed line* is the linear regression of the results. The position of M32 and NGC 4649 is indicated.

Table 3. Nuclear values of H_β , Mg_2 and $\langle Fe \rangle$ and solutions $\Delta \log(t)$, $\Delta \log(Z/Z_\odot)$, and $\Delta[Mg/Fe]$ for the galaxies of Gonzales (1993). The mean observational values are $\overline{H_\beta} = 1.75 \pm 0.009$, $\overline{Mg_2} = 0.32 \pm 0.001$, and $\langle Fe \rangle = 2.96 \pm 0.006$.

NGC	Mg_2	Fe_{52}	Fe_{53}	H_β	δMg_2	δH_β	$\delta \langle Fe \rangle$	$\Delta[Mg/Fe]$	$\Delta \log(Z/Z_\odot)$	$\Delta \log(t)$	M_B	M_V	Σ
221	0.216	2.99	2.66	2.36	-0.1005	-0.1357	0.6066	-0.4030	-0.1309	-0.3919	-15.70	-16.54	-
	0.004	0.04	0.04	0.05	0.004	0.029	0.051	0.0100	0.0102	0.0190			
224	0.340	3.39	3.17	1.82	0.0235	0.3193	0.0666	-0.0184	0.2022	-0.1156	-	-	-
	0.004	0.04	0.05	0.05	0.004	0.033	0.051	0.0103	0.0103	0.0190			
315	0.322	2.89	2.84	1.74	0.0055	-0.0957	-0.0134	0.0734	-0.0145	0.0030	-	-	-
	0.004	0.05	0.07	0.05	0.004	0.043	0.051	0.0115	0.0108	0.0190			
507	0.319	3.01	2.99	1.65	0.0025	0.0393	-0.1034	-0.0177	-0.0240	0.0963	-	-24.61	-
	0.006	0.09	0.11	0.07	0.006	0.071	0.071	0.0179	0.0158	0.0265			
547	0.324	2.98	2.66	1.67	0.0075	-0.1407	-0.0834	0.0973	-0.0503	0.0682	-	-	-
	0.004	0.06	0.07	0.06	0.004	0.046	0.061	0.0120	0.0122	0.0226			
584	0.294	3.11	2.84	2.10	-0.0225	0.0143	0.3466	-0.0867	0.0730	-0.2951	-21.72	-22.66	2.78
	0.004	0.04	0.03	0.04	0.004	0.029	0.041	0.0099	0.0190	0.0155			
636	0.283	3.24	2.89	1.93	-0.0335	0.1043	0.1766	-0.2088	-0.0113	-0.1068	-20.65	-21.57	1.48
	0.004	0.04	0.05	0.05	0.004	0.033	0.051	0.0103	0.0103	0.0190			
720	0.350	3.03	2.90	1.70	0.0335	0.0043	-0.0534	0.1712	0.0947	-0.0150	-21.60	-22.59	-
	0.006	0.12	0.14	0.12	0.006	0.092	0.120	0.0212	0.0231	0.0447			
821	0.327	3.20	2.87	1.73	0.0105	0.0743	-0.0234	0.0180	0.0479	0.0012	-21.61	-22.59	-
	0.004	0.05	0.05	0.05	0.004	0.036	0.051	0.0107	0.0105	0.0190			
1453	0.314	3.05	2.98	1.59	-0.0025	0.0543	-0.1634	-0.0588	-0.0624	0.1651	-	-	1.48
	0.004	0.05	0.07	0.05	0.004	0.043	0.051	0.0115	0.0108	0.0190			
1600	0.348	2.95	3.18	1.50	0.0315	0.1043	-0.2534	0.0891	0.0319	0.1845	-23.17	-24.14	-
	0.004	0.08	0.10	0.07	0.004	0.064	0.071	0.0145	0.0143	0.0263			
1700	0.293	3.20	2.88	2.09	-0.0235	0.0793	0.3366	-0.1242	0.0841	-0.2839	-22.28	-23.20	3.70
	0.004	0.05	0.05	0.05	0.004	0.036	0.051	0.0107	0.0105	0.0190			
2300	0.349	3.15	2.85	1.76	0.0325	0.0393	0.0066	0.1563	0.1269	-0.0723	-21.56	-22.60	2.85
	0.004	0.06	0.07	0.06	0.004	0.046	0.061	0.0120	0.0122	0.0226			
2778	0.349	3.05	2.71	1.76	0.0325	-0.0807	0.0066	0.2135	0.0921	-0.0712	-18.14	-19.05	-
	0.005	0.06	0.07	0.08	0.005	0.046	0.080	0.0137	0.0153	0.0300			
3377	0.287	2.82	2.53	2.07	-0.0295	-0.2857	0.3166	0.0152	-0.0510	-0.2488	-19.49	-20.39	1.48
	0.004	0.04	0.04	0.04	0.004	0.029	0.041	0.0099	0.0090	0.0155			
3379	0.336	3.07	2.78	1.65	0.0195	-0.0357	-0.1034	0.1092	0.0133	0.0627	-20.17	-21.13	0.00
	0.004	0.03	0.04	0.04	0.004	0.026	0.041	0.0096	0.0089	0.0155			
3608	0.330	3.00	2.82	1.73	0.0135	-0.0507	-0.0234	0.0937	0.0221	-0.0037	-19.87	-20.84	0.00
	0.005	0.05	0.06	0.07	0.005	0.039	0.071	0.0128	0.0138	0.0264			
3818	0.326	3.05	2.86	1.73	0.0095	-0.0057	-0.0234	0.0508	0.0213	0.0040	-19.49	-20.41	1.30
	0.006	0.07	0.07	0.07	0.006	0.050	0.071	0.0154	0.0148	0.0265			
4261	0.351	3.29	3.04	1.43	0.0345	0.2043	-0.3234	0.0493	0.0416	0.2464	-21.74	-22.73	1.00
	0.004	0.05	0.06	0.05	0.004	0.039	0.051	0.0111	0.0106	0.0190			
4278	0.330	2.76	2.67	1.48	0.0135	-0.2457	-0.2734	0.1570	-0.1405	0.2436	-19.79	-20.75	1.48
	0.004	0.04	0.05	0.05	0.004	0.033	0.051	0.0103	0.0103	0.0190			
4374 V	0.330	3.01	2.73	1.58	0.0135	-0.0907	-0.1734	0.0950	-0.0532	0.1440	-21.85	-22.73	2.30
	0.004	0.04	0.04	0.04	0.004	0.029	0.041	0.0099	0.0090	0.0155			
4472 V	0.326	3.03	3.15	1.72	0.0095	0.1293	-0.0334	-0.0148	0.0561	0.0126	-22.21	-23.19	-
	0.006	0.07	0.09	0.07	0.006	0.057	0.071	0.0163	0.0151	0.0265			
4478 V	0.287	2.99	2.80	1.87	-0.0295	-0.0657	0.1166	-0.1134	-0.0721	-0.0544	-19.44	-20.33	-
	0.004	0.05	0.05	0.06	0.004	0.036	0.061	0.0108	0.0117	0.0226			
4489	0.245	2.99	2.49	2.41	-0.0715	-0.2207	0.6566	-0.2009	-0.0336	-0.4987	-	-	-
	0.006	0.06	0.07	0.07	0.006	0.046	0.071	0.0151	0.0147	0.0265			
4552 V	0.362	3.07	3.06	1.54	0.0445	0.1043	-0.2134	0.1690	0.0975	0.1170	-	-21.68	2.00
	0.004	0.04	0.04	0.05	0.004	0.029	0.051	0.0100	0.0102	0.0190			
4649	0.376	3.10	3.22	1.38	0.0595	0.1993	-0.3734	0.1799	0.1057	0.2451	-21.81	-22.82	-
	0.004	0.04	0.06	0.04	0.004	0.037	0.041	0.0107	0.0093	0.0155			
4697 V	0.301	3.25	2.95	1.74	-0.0155	0.1393	-0.0134	-0.1514	-0.0193	0.0432	-21.51	-22.46	0.00
	0.006	0.06	0.06	0.07	0.006	0.043	0.071	0.0148	0.0145	0.0265			
5638	0.316	3.12	2.71	1.63	-0.0005	-0.0457	-0.1234	0.0043	-0.0675	0.1227	-	-	-
	0.004	0.04	0.05	0.04	0.004	0.033	0.041	0.0102	0.0091	0.0155			
5812	0.345	3.15	3.12	1.79	0.0285	0.1743	0.0366	0.0740	0.1648	-0.0949	-	-	-
	0.004	0.05	0.05	0.05	0.004	0.036	0.051	0.0107	0.0105	0.0190			
5813	0.318	2.95	2.60	1.48	0.0015	-0.1857	-0.2734	0.0640	-0.1648	0.2673	-	-	-
	0.004	0.06	0.07	0.06	0.004	0.046	0.061	0.0120	0.0122	0.0226			
5831	0.304	3.32	3.03	1.97	-0.0125	0.2143	0.2166	-0.1438	0.1105	-0.1894	-20.22	-21.85	3.60
	0.003	0.03	0.04	0.04	0.003	0.026	0.041	0.0080	0.0082	0.0153			
5846	0.339	3.03	2.84	1.60	0.0225	-0.0257	-0.1534	0.1147	0.0054	0.1056	-21.85	-22.84	0.30
	0.003	0.04	0.05	0.05	0.003	0.033	0.051	0.0088	0.0097	0.0189			
6127	0.331	2.95	2.82	1.52	0.0145	-0.0757	-0.2334	0.0861	-0.0708	0.2008	-	-	-
	0.006	0.07	0.08	0.06	0.006	0.053	0.061	0.0158	0.0138	0.0229			
6702	0.250	3.19	2.97	2.38	-0.0665	0.1193	0.6266	-0.3397	0.0695	-0.4824	-	-	-
	0.003	0.04	0.05	0.05	0.003	0.033	0.051	0.0088	0.0097	0.0189			
6703	0.292	3.10	2.82	1.97	-0.0245	-0.0007	0.2166	-0.1057	0.0065	-0.1633	-	-	-
	0.004	0.05	0.05	0.05	0.004	0.036	0.051	0.0107	0.0105	0.0190			
7052	0.337	2.95	2.82	1.40	0.0205	-0.0757	-0.3534	0.1041	-0.1009	0.3066	-	-	-
	0.004	0.06	0.07	0.06	0.004	0.046	0.061	0.0120	0.0122	0.0226			
7454	0.226	2.68	2.38	2.15	-0.0905	-0.4307	0.3966	-0.2336	-0.2708	-0.2031	-	-	-
	0.004	0.05	0.06	0.06	0.004	0.039	0.061	0.0112	0.0119	0.0226			
7562	0.304	3.09	2.71	1.74	-0.0125	-0.0607	-0.0134	-0.0400	-0.0668	0.0390	-	-	-
	0.003	0.04	0.04	0.04	0.003	0.029	0.041	0.0083	0.0083	0.0153			
7619	0.344	3.18	3.19	1.41	0.0275	0.2243	-0.3434	-0.0002	0.0146	0.2799	-22.35	-23.36	0.00
	0.003	0.04	0.05	0.03	0.003	0.033	0.031	0.0086	0.0073	0.0118			
7626	0.350	2.99	2.91	1.49	0.0335	-0.0107	-0.2634	0.1535	0.0013	0.1914	-22.36	-23.36	2.60
	0.003	0.03	0.04	0.04	0.003	0.026	0.041	0.0080	0.0082	0.0153			
7785	0.307	3.02	2.95	1.63	-0.0095	0.0243	-0.1234	-0.0774	-0.0785	0.1402	-22.22	-23.18	-
	0.003	0.04	0.05	0.05	0.003	0.033	0.051	0.0088	0.0097	0.0189			

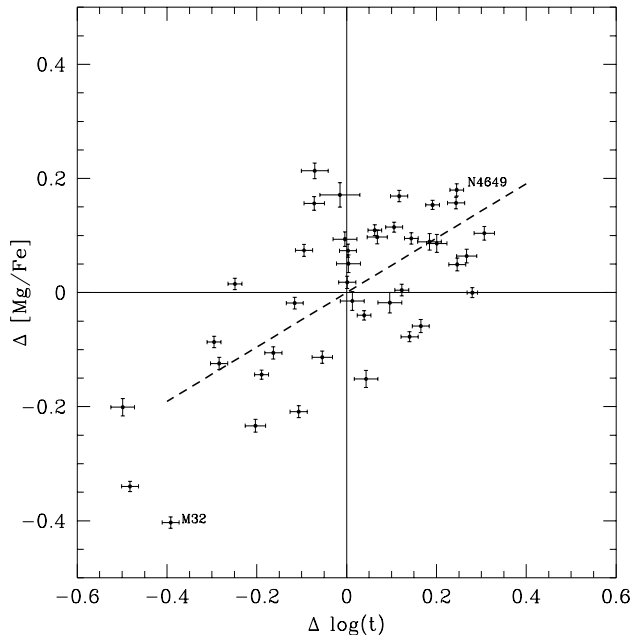


Fig. 6. The $\Delta[\text{Mg}/\text{Fe}]$ versus $\Delta \log(t)$ relation. The *thick dashed line* is the linear regression of the results. The position of M32 and NGC 4649 is indicated.

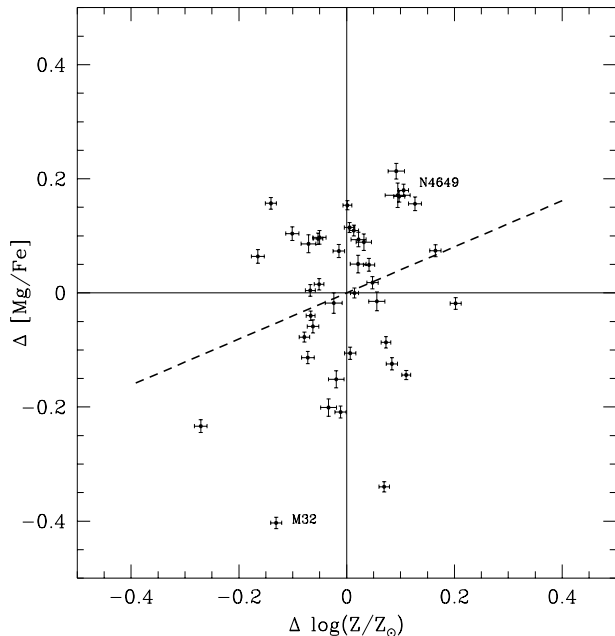


Fig. 7. The $\Delta[\text{Mg}/\text{Fe}]$ versus $\Delta \log(Z/Z_{\odot})$ relation. The *thick dashed line* is the linear regression of the results. The position of M32 and NGC 4649 is indicated.

of star formation and chemical enrichment, and the mechanism of galaxy formation as well.

Before starting this part of the analysis it is worth clarifying the real meaning of the *age* parameter $\Delta \log(t)$. This age (being mainly revealed by H_{β}) actually refers to the younger components of the stellar mix in the galaxy (nucleus). In the ideal case (however possible) of continuous star formation from the early epochs it would measure the overall duration of the star forming activity. In the case that recurrent episodes have taken place (such as in mergers and/or bursts), it would measure the age of the last episode. Given these premises, we examine the following relationships:

Age-Z. The relation between $\Delta \log(Z/Z_{\odot})$ and $\Delta \log(t)$ is shown in Fig. 5, where only a large scatter is seen (no systematic trend). The degree of metal enrichment seems to be totally unrelated to the age, in the sense that at any given metallicity all ages are possible. Does it mean that sporadic episodes of star formation may change the age parameter without significantly affecting the metallicity? It is worth recalling that H_{β} is very sensitive to recent star formation, and that a burst of stellar activity implying even a very small fraction of the galaxy mass would immediately increase H_{β} without affecting the metallicity (cf. Bressan et al. 1996). Furthermore, the recovery time of H_{β} after a burst is of order of about 1 Gyr, after which no trace of the star forming period would be easily detectable with the H_{β} diagnostic.

Age-[Mg/Fe]. The relationship between $\Delta[\text{Mg}/\text{Fe}]$ and $\Delta \log(t)$ is shown in Fig. 6. Now a good relation is found: older galaxies seem to be more enhanced in α -elements.

Z-[Mg/Fe]. The relationship between $\Delta[\text{Mg}/\text{Fe}]$ and $\Delta \log(Z/Z_{\odot})$ is shown in Fig. 7. It appears that more metal-rich galaxies are likely to also more enhanced in α -elements.

In order to cast light on the physical implications of the above relations, we separately correlate $\Delta \log(t)$, $\Delta \log(Z/Z_{\odot})$, and $\Delta[\text{Mg}/\text{Fe}]$ to the total luminosity of the galaxy as measured by the absolute magnitude M_V . The discussion below will not change using M_B . The three relations are shown in Fig. 8 (age), 9 (metallicity), and 10 ($[\text{Mg}/\text{Fe}]$).

Age- M_V . Inspecting the distribution of galaxies in Fig. 8 two features can be noticed in spite of the large scatter:

- First in our sample all galaxies but M32 are brighter than $M_V = -20$, which is the range of the classical color-magnitude relation of Bower et al. (1992).
- Second there seems to be a sort of upper limit to $\Delta \log(t)$ set by the following group of galaxies, namely NGC 2778, NGC 3818, NGC 3379, NGC 4552, NGC 4649, NGC 4261, and NGC 7619, to which NGC 4478, NGC 3608 and NGC 4374 can perhaps be

added. There is one exception though, represented by NGC 4278, which appears to be either too old for its luminosity or too faint for its age.

As far as the suggest age is concerned, it is worth noticing that three galaxies of this group, namely NGC 4374, NGC 4478, and NGC 4552, belong to the Virgo cluster (so that their distance and magnitude are less of a problem in this context) and have $\Sigma \leq 2$, which according to Sweitzer & Seitzer (1992) means mild rejuvenation and/or interaction. The remaining galaxies of this sub-group have either $\Sigma \leq 1.5$ or missing. Finally, the last Virgo galaxy in our sample, namely NGC 4697, deviates from the relation defined by its companions in spite of its similar M_V and no signs of interaction (Sweitzer and Seitzer 1992).

If the above limit is real and not caused by statistical effects due to scarce population of galaxies under consideration, it implies that the last episode of star formation occurred earlier and earlier at increasing luminosity (likely mass of the galaxy). Is this the locus of non-interacting galaxies, along which we see the pristine star formation? If so, recalling the meaning of the age parameter in usage here this implies that star formation either started later or continued longer at decreasing galaxy mass (cf. Bressan et al. 1996 for a similar suggestion).

All other galaxies are much scattered along the age axis. Indeed most of them have sign of interaction or rejuvenation (Sweitzer & Seitzer 1992). Does it imply that more recent star formation has occurred altering H_β and age assignment in turn ?

M32 is an ambiguous case because either it could represent the continuation of the trend shown by the old galaxies, in which star formation lasted till a recent past or it could have been rejuvenated by a recent episode. As compared to NGC 4649 there is factor 4.0 in between. Assuming the canonical age of 15 Gyr for the oldest galaxies, M32 terminated its star formation history or suffered from star formation about 3.75 Gyr ago. The possibility that M32 contains a significantly younger stellar component is also indicated by studies of the classical color-magnitude diagram (CMD) of the resolved stars. Although care must be paid because those CMD do not refer to the central region of M32, an age of $4 \div 5$ Gyr was estimated by Freedman (1989) and Freedman (1992). See also Elston & Silva (1992), Davidge & Jones (1992), and Hardy et al. (1994) for similar conclusions. Based on the population synthesis technique and the mean colors of M32, O’Connell (1988 and references therein) suggested an age of about 6 Gyr. Along the same vein Bressan et al. (1994) argued that the bulk of stars have ages as old as those typical of globular clusters say in the range $13 \div 15$ Gyr, with a younger component which cannot be older than 5 Gyr and younger than 1 Gyr. This latter boundary is set by the UV properties of M32 which has $(1550-V)=4.5$ (Burstein et al. 1988). Remarkably, this estimate is consistent with the recent study by Grillmair et al. (1996) of a field in M32 taken at the distance of about $2 \times R_e$, who find that the CMD

of this region is consistent with a luminosity weighted age of about 8.5 Gyr and $[Fe/H]=-0.25$, however with some evidence for another component with $[Fe/H]=0$ for which younger ages cannot be excluded. As far as the very central part of M32 is concerned, an independent estimate of the age is still missing to our knowledge.

$Z-M_V$. The relationship between $\Delta \log(Z/Z_\odot)$ and M_V is shown in Fig. 9. According to the best fit of the data (thick dashed line) the metallicity seems to weakly increase with the luminosity (mass) of the galaxy. Limiting the inspection to the group of galaxies that were used to argue about the age limit in Fig. 8, all but NGC 4478 (and M32) are more metal-rich than the mean value of the sample but showing no particular trend with the luminosity.

Worth noticing is the case of all galaxies brighter than $M_V = -20$ and apparently younger than the mean age (cf. Fig. 8) whose metallicity is in contrast above the mean value (but for NGC 3377 whose $\Delta \log(Z/Z_\odot) \simeq 0$). The remaining objects scatter above and below the mean value. Does this suggests that galaxies suffering from subsequent episodes of star formation have further increased their metallicity ? Furthermore, we call attention on NGC 507, the brightest galaxy in the sample, which has age and metallicity only slightly below and above the mean, respectively.

Going back to the apparent lack of a positive correlation between metallicity and luminosity, if we consider only those objects of the age group that are also members of the Virgo cluster and therefore distance and absolute magnitudes are less of a problem (namely NGC 4374, NGC 4478, and NGC 4552) they seem to be more metal-rich at increasing luminosity.

Does the above inspection imply that the canonical trend “metallicity increasing with the luminosity” holds only for galaxies at rest (provided that the their absolute luminosity is well determined) ? And in all other cases the relation is blurred by recent stellar activity and/or uncertainties in their absolute magnitudes ? More data are required to answer this question.

$[Mg/Fe]-M_V$. Fig. 10 shows the relation between $\Delta[Mg/Fe]$ and M_V . We start noticing that with the exception of NGC 4478 (and M32), all other galaxies of the group defining the age limit in Fig. 8 are more enhanced in α -elements than the mean value of the sample, whereas the remaining galaxies scatter below and above it. It appears that not necessarily galaxies with high metallicity are also enhanced in α -elements, even if from the results shown in Fig. 7 some trend of this kind should hold on a broad sense. Furthermore, galaxies whose nuclear age is below the mean value not necessarily are more enhanced in α -elements. This can perhaps be explained recalling that star formation over periods of time longer than about 1 Gyr easily wipes out the signature type II supernovae in the abundance ratio $[\alpha/Fe]$. As far as the expectation that

$[\text{Mg}/\text{Fe}]$ increases with the galaxy luminosity is concerned, no such relation is noticed at a first sight. However, restricting ourselves only to galaxies members of the age limit group and of the Virgo cluster (namely NGC 4374, NGC 4478, and NGC 4552), the above trend is recovered. The same considerations made for the Z - M_V plane apply also to this case.

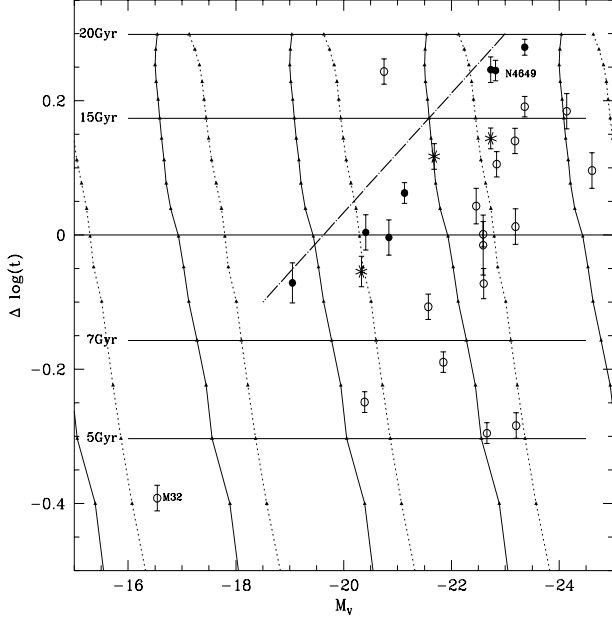


Fig. 8. The $\Delta \log(t)$ versus M_V relation. Filled circles are the galaxies defining the age limit (see the text for details), the heavy stars are the three galaxies of this group belonging to the Virgo cluster, and the open circles are all remaining galaxies. The *eye drawn long-dashed-dotted line* is only meant to visualize the age limit. Finally, the position of M32, NGC 4649 is indicated. Superposed to this diagram is are the fading lines of SSPs: the thin dotted and solid lines are for $Z=0.004$ and $Z=0.05$, respectively; each dot along the lines show the age in step of 1 Gyr starting from 20 Gyr (top) down to 4 Gyr (bottom); the thin horizontal lines locate the loci of constant age (20, 15, 10, 7, and 5 Gyr starting from the top). Finally, the fading lines of SSP (in pairs because of the different metallicity) are shown for different values of the total mass, namely 10^{12} , 10^{11} , 10^{10} , 10^9 , and $10^8 \times M_\odot$ from right to left.

8. Towards absolute ranking: an attempt

Having established the relative differences $\Delta \log(t)$, $\Delta \log(Z)$, and $\Delta[\text{Mg}/\text{Fe}]$ from galaxy to galaxy, the absolute ranking of the central regions of different galaxies can be attempted. The main problem is with the zero point of the age, metallicity and enhancement scale. We take M32 as the reference object. As already mentioned several observational hints concur to suggest that M32 likely suffered

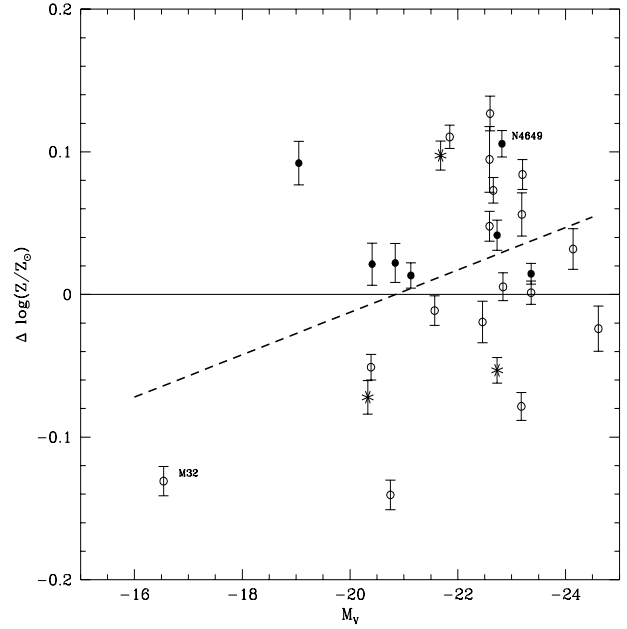


Fig. 9. The $\Delta \log(Z/Z_\odot)$ versus M_V relation. The *thick dashed line* is the linear regression of the results. Filled circles are the galaxies defining the age limit (see the text for details), the heavy stars are the three galaxies of this group belonging to the Virgo cluster, and the open circles are all remaining galaxies. Finally, the position of M32, NGC 4649 is indicated.

from an episode or continued to form stars as recently as $4 \div 5$ Gyr ago (Freedman 1992). As far as the metallicity is concerned, it seems to span a wide range. The lower limit in Freedman (1989) is $[\text{M}/\text{H}]=-0.5$ with a upper limit up to $[\text{M}/\text{H}]=0.1$ or even higher than that according to Bica et al. (1991). There is no direct indication of $[\text{Mg}/\text{Fe}]$ (at least to our knowledge). For the purposes of the present discussion, we adopt as zero points: 4 Gyr for the age, $[\text{Mg}/\text{Fe}]_{\text{M32}} = 0$ for the enhancement in α -elements, and $[\text{Fe}/\text{H}]_{\text{M32}} = -0.25$ for the iron content or with the aid of equation (1), in which the term (X/X_\odot) is neglected and $Z_\odot = 0.016$, $Z_{\text{M32}} = 0.0128$. The absolute values assigned to the age, metallicity, and $[\text{Mg}/\text{Fe}]$ of all other galaxies in the sample can be easily re-scaled if the zero point is going to change.

The age is assigned with the aid of grids of SSP as drawn in Fig. 8: the thin dotted and solid lines are for $Z=0.004$ and $Z=0.05$, respectively; each dot along the lines show the age in step of 1 Gyr starting from 20 Gyr (top) down to 4 Gyr (bottom); the thin horizontal lines locate the loci of constant age (20, 15, 10, 7, and 5 Gyr starting from the top). Finally, the fading lines of SSP (in pairs because of the different metallicity) are shown for different values of the total mass, namely 10^{12} , 10^{11} , 10^{10} , 10^9 , and $10^8 \times M_\odot$ from right to left. The metallicity and $[\text{Mg}/\text{Fe}]$

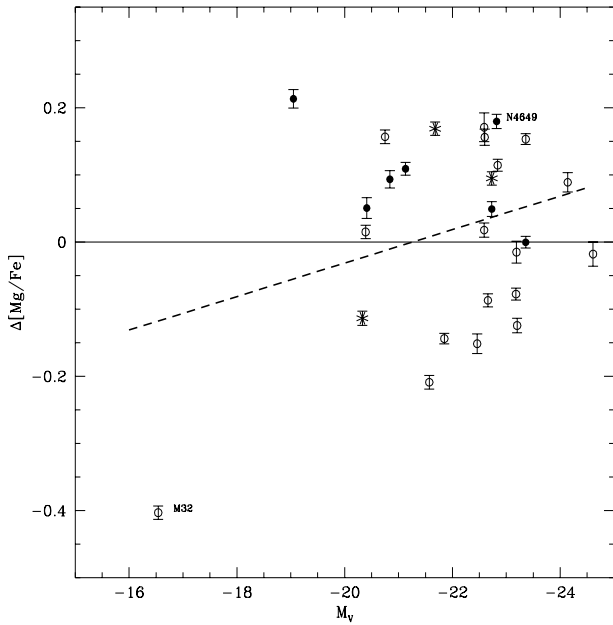


Fig. 10. The $\Delta[\text{Mg}/\text{Fe}]$ versus M_V relation. The *thick dashed line* is the linear regression of the results. Filled circles are the galaxies defining the age limit (see the text for details), the heavy stars are the three galaxies of this group belonging to the Virgo cluster, and the open circles are all remaining galaxies. Finally, the position of M32, NGC 4649 is indicated.

are assigned by simply shifting the vertical axis in Figs. 9 and 10.

The results are summarized in Table 7 limited to the group of galaxies that in Fig. 8 define the age boundary.

9. Isolation or mergers?

The fading lines in Fig. 8 help to visualize in the age-magnitude diagram the path followed by an evolving galaxy under a number of different scenarios. Perhaps the most intriguing question to address about galaxies is which of the two main avenues for their formation and evolution has prevailed as the dominant mechanism, i.e. isolation or mergers.

If a galaxy forms and evolves in isolation, and suffers from a number of episodes of star formation (from one to several or even continuous) it would simply slide up and down along its fading line according to the stage of stellar activity at which the galaxy is detected with little transversal shift caused by chemical enrichment. Complications due to the possible presence of gas can be neglected here. As already said the data are compatible with this scheme suggesting that there are two groups of galaxies: those with no sign of rejuvenation in which either the overall duration or the epoch of the last episode of star formation seems to go inversely proportional to the galaxy

Table 4. Estimated ages, metallicities, and enhancements of α -elements for the group of galaxies defining the old age edge in Fig. 17

NGC	Age	$\langle Z \rangle$	$[\text{Mg}/\text{Fe}]$
221	4.0	0.0128	0.00
2778	8.4	0.0216	0.62
3379	11.4	0.0180	0.51
3608	10.0	0.0184	0.49
3818	10.0	0.0184	0.46
4261	17.4	0.0193	0.45
4374	14.0	0.0245	0.49
4478	9.0	0.0150	0.28
4552	12.9	0.0219	0.57
4649	17.3	0.0224	0.58
7619	18.8	0.0181	0.42

mass, and those with signs of rejuvenation which are obviously scattered in this diagram.

The case of hierarchical merging is more difficult to discuss because the path is determined by the mass and evolutionary stage of the merging galaxies, and the amount of star formation taking place during the merger event. Let us suppose for the sake of simplicity that two identical units (same age, same composition, and say $10^{10} \times M_\odot$ mass each) merge triggering star formation in the composite system. The resulting galaxy will brighten by 0.75 magnitude because of the increased mass, shift to the line for the new total mass, slide down along this because of star formation, and slightly redden because of the increased metallicity (passing from $Z=0.001$ to $Z=0.05$ the magnitude decrement is $\Delta M_V = 1.0$ at most). The total displacement vector depends on the relative amount of gas turned into stars. In any case, the displacement will be nearly vertical along the $2 \times 10^{10} M_\odot$ line in our example. As soon as star formation is over, the galaxy will fade at slowing rate back to a point near the original position. It is worth recalling that the recovery time after a burst of stellar activity is short (going from a few 10^8 yr to 1 Gyr at most). In principle there is no contradiction between this scenario and the bunch of galaxies scattered in this diagram toward much younger ages. The problem is with they recovering position if this latter corresponds to the group of galaxies with no sign of rejuvenation. Indeed if the seed galaxies had the same age we would expected the daughter galaxies to cluster along a nearly horizontal line in this diagram. In contrast, it seems as if bright, high mass galaxies had their merger adventure long ago, whereas the faint, low mass objects did it in a more recent past, but starting from seed galaxies with small stellar content. This

is equivalently to say that the bulk of star forming activity took place more and more toward the present at decreasing mass of the galaxy. Furthermore, *why do not we see in this diagram any low mass galaxy (the potential seeds of a bigger galaxy in the hierarchical scheme) at the same age range of the big galaxies ? Is this only due to selection effects in our sample (because no dwarf galaxies but M32 are present) or more subtle causes are to be considered?* As nowadays answering this question is difficult owing to the lack of sufficient data with precise measurements of $H\beta$, Mg_2 and $\langle Fe \rangle$.

10. SN-driven winds or variable IMF?

To explain the color-magnitude relation (CMR) of early type galaxies, colors get redder at increasing luminosity (cf. Bower et al. 1992 for the case of the Virgo and Coma galaxies), long ago Larson (1974) postulated that it is the consequence of SN-driven galactic winds. In the classical scenario, isolation and constant IMF, massive galaxies eject their gaseous content much later and get higher mean metallicities than the low mass ones. The implication is that the global duration of the star forming activity is proportional to the galaxy mass. The alternative of the CMR being an age sequence in the sense that blue galaxies have started star formation much later than in red ones has been proved to disagree with the redshift evolution of early type galaxies in the HST Deep Field (cf. Kodama & Arimoto 1996).

As already recalled, bright ellipticals seem to be more enhanced in α -elements than the faint ones (cf. section 1). The simplest interpretation of the α -enhancement problem (cf. Matteucci 1997 for a recent review of the subject), as a result of the different time scale for contaminating the galactic gas by the products of the short-lived Type II supernovae (main producer of α -elements) and the long-lived Type I supernovae (main producers of Fe) via the mass accreting white dwarfs mechanism, requires that the overall duration of the star forming activity is short in massive ellipticals and long in the low-mass ones, just the opposite of what implied by the CMR. This has long been a point of embarrassment of the standard SN-driven galactic wind model.

The present analysis seems to lead to a more complex scenario in which the trends implied by the CMR and enhancement in α -elements are perhaps simultaneously recovered only for galaxies at *rest* (provided their magnitudes are well determined), whereas in all other cases, in which $H\beta$ and Σ indicate signatures of recent stellar activity, rejuvenation and/or interactions, the above key relations are blurred by side effects hard to quantify.

In any case, all galaxies of the age limit group but for NGC 4478 are more enhanced in α -elements with respect to the mean, whereas all the others scatter both below and above it. Similar considerations apply to the metallicity.

Taken as face values, the results of our analysis weaken the classical SN-driven wind model based on monolithic star formation with constant IMF and isolation. However, as examined in the previous section, even the pure merger scenario has some intrinsic difficulties with the distribution of galaxies in the age-luminosity plane.

A viable scheme suggested by the present results is one in which all galaxies have begun to form stars at the same time but, depending on their mass, the process has continued (maybe in discrete episodes) over different periods of time. Massive galaxies did it in the far past and the star forming period ceased very soon. Low mass galaxies started at the same epoch, but continued for longer periods of time (the duration increasing at decreasing galactic mass). Subsequently, galaxies of any luminosity (mass) may have undergone additional episodes of star formation, depending on circumstances that cannot be singled out by this kind of analysis, which reflect themselves in the large dispersion in the age- M_V plane. As far as the metallicity and enhancement in α -elements are concerned, although the tendency to increase with the galaxy luminosity (mass) can be noticed in the case of inactive galaxies, as required by the CMR α -enhancement problem, it seems as if each galaxy had its own individual history of enrichment in heavy and α -elements.

An attempt to break the contradictions of the standard SN-driven galactic wind model has recently been made by Chiosi et al. (1997) who have calculated new models of elliptical galaxies with variable IMF. To this aim they adopted the IMF by Padoan et al. (1997), which depends on the density, temperature and velocity dispersion of the medium in which stars are formed. In brief, in a hot, rarefied medium the Padoan et al. (1997) IMF is more skewed towards the high mass end than in a cool, dense medium. This kind of situation is met passing from a high mass (low mean density) to a low mass (high mean density) galaxy or from the center to the periphery of a given galaxy. The models based on this IMF can account for a number of observed chemical and photometric constraints for elliptical galaxies. In fact, they predict the onset of galactic winds and consequent termination of the star forming period earlier in massive galaxies than in the low mass ones. The reason of it resides in the skewness of the IMF toward the high mass end that changes with the mean gas density (galactic mass and/or position within a galaxy) thus favoring in massive galaxies the relative percentage of SN explosions and consequent heating of the gas to the escape velocity. In this scheme massive galaxies despite their short duration of stellar activity yet reach high metallicities and $[Mg/Fe]$ ratios. The opposite occurs in the low mass ones. Unfortunately, Scalo et al. (1997) have strongly questioned the Padoan et al. (1997) IMF, thus weakening the foundations of the Chiosi et al. (1997) scenario. However, according to Scalo et al. (1997) other model IMF could be constructed to give similar dependences. Whether they would also lead to model galaxies

like those by Chiosi et al. (1997) cannot be said. All the problems are still there!

11. Conclusions

In this study we have investigated the ability of the H_β , Mg_2 and $\langle Fe \rangle$ diagnostics to assess the metallicity, $[Mg/Fe]$ ratios, and ages of elliptical galaxies. First, we have tried to interpret the gradients in H_β , Mg_2 and $\langle Fe \rangle$ across individual galaxies. Second, we have tackled the problem of the information hidden in the different values of H_β , Mg_2 , and $\langle Fe \rangle$ observed in the nuclear regions of elliptical galaxies. The results of this study can be summarized as follows:

1. We provide basic calibrations for the variations δH_β , δMg_2 and $\delta \langle Fe \rangle$ as a function of variation in age $\Delta \log(t)$, metallicity $\Delta \log(Z/Z_\odot)$, and $\Delta [Mg/Fe]$ of SSPs whose application is of general use.
2. Limited to a small sample of objects for which the observational data are available, we analyze from a quantitative point of view how the difference δH_β , δMg_2 , and $\delta \langle Fe \rangle$ between the external and central values of each index translates into $\Delta [Mg/Fe]$, $\Delta \log(Z/Z_\odot)$, and $\Delta \log(t)$. We find that out of six galaxies under examination, four have the nuclear region more metal-rich, more enhanced in α -elements, and younger (i.e. containing a significant fraction of stars of relatively young age) than the external regions. In contrast the remaining two galaxies have the nuclear region more metal-rich, more enhanced in α -elements but marginally older than the external zones. Whether this dichotomy in the age difference between the central and the external regions is a rule is difficult to assess at the present time owing to the very small number of objects for which the analysis has been feasible. Such a possibility has been envisaged by Bressan et al. (1996). We intend to reconsider the whole problem in a forthcoming paper utilizing the 20 galaxies of the Gonzales (1993) catalog for which gradients are available.
3. The above calibration is used to explore the variation from galaxy to galaxy of the nuclear values of H_β , Mg_2 , and $\langle Fe \rangle$ limited to a sub-sample of the Gonzales (1993) list. The differences δH_β , δMg_2 , and $\delta \langle Fe \rangle$ are converted into the differences $\Delta \log(t)$, $\Delta \log(Z/Z_\odot)$, and $\Delta [Mg/Fe]$. Various correlations among the age, metallicity, and enhancement variations are explored. In particular we thoroughly examine the relationships $\Delta \log(t) - M_V$, $\Delta \log(Z/Z_\odot) - M_V$, and $\Delta [Mg/Fe] - M_V$. It is found that a sort of age limit is likely to exist in the $\Delta \log(t) - M_V$ plane, traced by galaxies with mild or no sign of rejuvenation. In these objects, the duration of the star forming activity is likely to have increased at decreasing galactic mass. Limited to these galaxies and provided the luminosity is well determined, the

mass-metallicity sequence implied by the CMR is recovered, likewise for the α -enhancement-luminosity relation suggested by the gradients in Mg_2 and $\langle Fe \rangle$. For the remaining galaxies the situation is more intriguing: sporadic episodes of star formations are likely to have occurred scattering the galaxies in the space of age, metallicity, and $[Mg/Fe]$. The results are discussed in regard to predictions from the merger and isolation models of galaxy formation and evolution highlighting points of difficulty with each scheme. Finally, the suggestion is advanced that models with an IMF that favors higher mass stars in massive elliptical galaxies, and lower mass stars in low-mass ellipticals, might be able to alleviate some of the difficulties encountered by the standard SN-driven galactic wind model and lead to a coherent interpretation of the data.

Acknowledgements. We deeply thank Dr. Guy Worthey for his constructive referee report. His remarks greatly improved the original version of the paper. This study has been financed by the Italian Ministry of University, Scientific Research and Technology (MURST), the Italian Space Agency (ASI), and the TMR grant ERBFMRX-CT96-0086 from the European Community.

References

- Anders E., & Grevesse N., 1989, *Geochim. Cosmochim. Acta* 53, 197
- Arimoto N., Yoshii Y. 1987, *A&A* 173, 23
- Barbuy B. 1994, *ApJ* 430, 218
- Bertelli G., Bressan A., Chiosi C., Fagotto F., Nasi E. 1994, *A&AS* 106, 275
- Bertin G., Saglia R.P., Stiavelli M. 1992, *ApJ* 384, 423
- Bica E., Barbuy B., Ortolani S. 1991, *ApJ* 382, L15
- Borges A.C., Idiart T.P., De Freitas Pacheco J.A., Thevenin F. 1995, *AJ* 110, 2408
- Bower R.G., Lucey J.R., Ellis R.S. 1992, *MNRAS* 254, 589
- Bressan A., Chiosi C., Fagotto F. 1994, *ApJS* 94, 63
- Bressan A., Chiosi C., Tantalo R. 1996, *A&A* 311, 425
- Bressan A., Girardi L., Chiosi C. 1997, in preparation
- Burstein D., Bertola F., Buson L.M., Faber S.M., Lauer T.R. 1988, *ApJ* 328, 440
- Carollo C.M., Danziger I.J., Buson L. 1993, *MNRAS* 265, 553
- Carollo C.M., Danziger I.J. 1994a, *MNRAS* 270, 523
- Carollo C.M., Danziger I.J. 1994b, *MNRAS* 270, 743
- Chiosi C., Bressan A., Portinari L., Tantalo R. 1997, *A&A* submitted
- Davidge T.J., Jones J.H. 1992, *AJ* 104, 1365
- Davies R.L., Sadler E.M., Peletier R. 1993, *MNRAS* 262, 650
- De Freitas Pacheco J.A. 1997, *A&A* 319, 394
- Elston R., Silva D.R. 1992, *AJ* 104, 1360
- Faber S.M., Worthey G., Gonzales J.J. 1992, in *IAU Symp.* 149, B. Barbuy and A. Renzini (eds.), p.255
- Fisher D., Franx M., Illingworth G. 1996, *ApJ* 459, 110
- Fisher D., Franx M., Illingworth G. 1995, *ApJ* 448, 119
- Freedman W.L. 1989, *AJ* 98, 1285
- Freedman W.L. 1992, *AJ* 104, 1349
- Gibson B.K. 1996, *MNRAS*, submitted
- Gibson B.K. 1994, *MNRAS* 271, L35

- Gonzales J.J. 1993, Ph.D. Thesis, Univ. California, Santa Cruz
- Grevesse N., 1991, A&A 242, 488
- Grevesse N., Noels A., 1993, Phys. Scr. T. 47, 133
- Grillmair C.J., Lauer T.R., Worthey G., et al. 1996, AJ 112, 1975
- Hardy E., Couture J., Couture C., Joncas G. 1994, AJ 107, 195
- Idiart T.P., de Freitas Pacheco J.A. 1995, AJ 109, 2218
- Idiart T.P. & de Freitas Pacheco J.A. 1997, The 38th Hermonceaux Conference: The Initial Mass Function, in press
- Iglesias C.A., Rogers F.J. 1993, ApJ, 412, 752
- Kodama T., Arimoto N. 1997, A&A in press
- Larson R.B. 1974, MNRAS 166, 585
- Matteucci F. 1997, Fund. Cosmic Phys. 17, 283
- O’Connell R.M. 1988, in Starbursts and Galaxy Evolution, ed. T.X. Thuan, T. Montmerle, & J. Tran Than Van p. 367. Gif-sur Yvette: Editions Frontieres.
- Padoan P., Nordlund A.P., Jones B.J.T. 1997, MNRAS, 288, 145
- Portinari L., Chiosi C., Bressan A. 1997, A&A to be submitted
- Scalo J., Vazquez-Semadeni E., Chappell D., Passot T., 1991, ApJ, submitted (astro-ph/9710075)
- Schweizer F., Seitzer P. 1992, AJ 104, 1039
- Tantalo R., Bressan A., Chiosi C. 1997, A&A, submitted
- Tantalo R., Chiosi C., Bressan A., Fagotto F. 1996, A&A 311, 361
- Thielemann F.K., Nomoto K., Hashimoto M. 1993, in *The Origin and Evolution of Elements*, ed. N. Prantzos et al. p. 297, Cambridge: Cambridge Univ. Press
- Thielemann F.K., Nomoto K., Hashimoto M. 1996, ApJ 460, 408
- Weiss A., Peletier R.F., Matteucci F. 1995, A&A 296, 73
- Worthey G. 1992, Ph.D. Thesis, Univ. California, Santa Cruz
- Worthey G., 1994, ApJS 95, 107
- Worthey G., Faber S.M., Gonzales J.J., Burstein D. 1994, ApJS 94, 687
- Young P.J. 1976, AJ 81, 807

This article was processed by the author using Springer-Verlag L^AT_EX A&A style file L-AA version 3.



